A Unified Position Analysis of the Dixon and the Generalized Peaucellier Linkages

Nicolas Rojas[a], Aaron M. Dollar[a], Federico Thomas[b,*]

[a]Department of Mechanical Engineering and Materials Science, Yale University, New Haven, CT, USA
[b]Institut de Robòtica i Informàtica Industrial (CSIC-UPC), Llorens Artigas 4-6, 08028 Barcelona, Spain

Abstract

This paper shows how, using elementary Distance Geometry, a closure polynomial of degree 8 for the Dixon linkage can be derived without any trigonometric substitution, variable elimination, or artifice to collapse mirror configurations. The formulation permits the derivation of the geometric conditions required in order for each factor of the leading coefficient of this polynomial to vanish. These conditions either correspond to the case in which the quadrilateral defined by four joints is orthodiagonal, or to the case in which the center of the circle defined by three joints is on the line defined by two other joints. This latter condition remained concealed in previous formulations. Then, particular cases satisfying some of the mentioned geometric conditions are analyzed. Finally, the obtained polynomial is applied to derive the coupler curve of the generalized Peaucellier linkage, a linkage with the same topology as that of the celebrated Peaucellier straight-line linkage but with arbitrary link lengths. It is shown that this curve is 11-circular of degree 22 from which the bicircular quartic curve of the Cayley's scalene cell is derived as a particular case.

Keywords: Dixon linkage, scalene cell, Peaucellier linkage, generalized Peaucellier linkage, coupler curves, position analysis, Distance Geometry, distance-based kinematics.

*Corresponding author. Tel.: +34 934015757; fax: +34 934015750.
Email addresses: nicolas.rojas@yale.edu (Nicolas Rojas), aaron.dollar@yale.edu (Aaron M. Dollar), fthomas@iri.upc.edu (Federico Thomas)

Notation

P_i	point i in some Euclidean space
$\mathbf{p}_i$	position vector of point P_i in the global reference frame
$\mathbf{p}_{i,j} = \mathbf{p}_j - \mathbf{p}_i$	vector pointing from P_i to P_j
$d_{i,j} = \|\mathbf{p}_j - \mathbf{p}_i\|$	distance between P_i and P_j
$s_{i,j} = \|\mathbf{p}_j - \mathbf{p}_i\|^2$	squared distance between P_i and P_j
$\mid_{i,j}$	line segment connecting P_i and P_j
$\wedge_{i,j,k}$	the dyad defined by the segments $\mid_{i,j}$ and $\mid_{j,k}$
$\triangle_{i,j,k}$	triangle defined by P_i, P_j, and P_k
$A_{i,j,k}$	oriented area of $\triangle_{i,j,k}$ in $\mathbb{E}^2$
$\square_{i,j,k,l}$	quadrilateral with diagonals $\mid_{i,k}$ and $\mid_{j,l}$
$\diamondsuit_{i,j,k,l,m}$	three dyads, $\wedge_{i,j,m}$, $\wedge_{i,k,m}$, and $\wedge_{i,l,m}$, sharing their end-points

1. Introduction

The Dixon linkage, named after Alfred Dixon who first studied it in 1900 [1], is a planar nine-bar linkage with three triple joints. Its topology is that of a hexagon with three diagonals, the ones whose end points belong to non-consecutive edges [Fig. 1(left)]. By applying Laman's theorem [2], it can be verified that this linkage is, in general, rigid. Conditions under which it becomes movable were studied by Dixon [1], Wunderlich [3], and more recently by Stachel [4]. In 2007, Walter and Husty obtained the univariate closure polynomial of this linkage in its completely general form (that is, without explicitly specifying the eight bar lengths) [5]. Using a substitution based on a complex parametrization of the unit circle to eliminate the trigonometric functions, and a sequence of elaborated eliminations, they were able to obtain a polynomial of degree 16 with 2.770.936 monomials. Then, this polynomial was reduced to order 8 by collapsing mirror configurations into single configurations. This proved that the Dixon linkage has at most 8 assembly modes for a given set of link lengths thus proving a conjecture by Wunderlich.

In this paper, we show how, using Distance Geometry, a closure polynomial for the Dixon linkage, of degree 8 with 1.018.150 monomials, can be directly derived without any trigonometric substitution, variable elimination, polynomial factorization, or artifice for collapsing mirror configurations.

A general technique to obtain closure polynomials for arbitrary planar linkages using Distance Geometry was presented in [6]. This technique relies on the use of the so-called bilateration matrices. The use of this kind of matrices is useful when the linkage to be analyzed contains ternary links (that is, triangles whose orientation is imposed). Nevertheless, when analyzing linkages with only binary links, a more direct and simpler approach can in general be adopted. This is the case of the Dixon linkage for which a simple ad-hoc derivation is presented herein.

The general Dixon linkage is minimally rigid, that is, when one of its links is removed, the mechanism gains one degree of mobility. Actually, if we eliminate any link in the Dixon linkage we obtain the generalized Peaucellier linkage, that is, a linkage with the topology of the standard Peaucellier linkage [Fig. 1(right)] [7, Chapter 8], but without constraints relating its link lengths. For example, if we eliminate the link connecting P_1 and P_6 and we fix the location of P_1 and P_6 in the Dixon linkage shown in Fig. 1(left), we

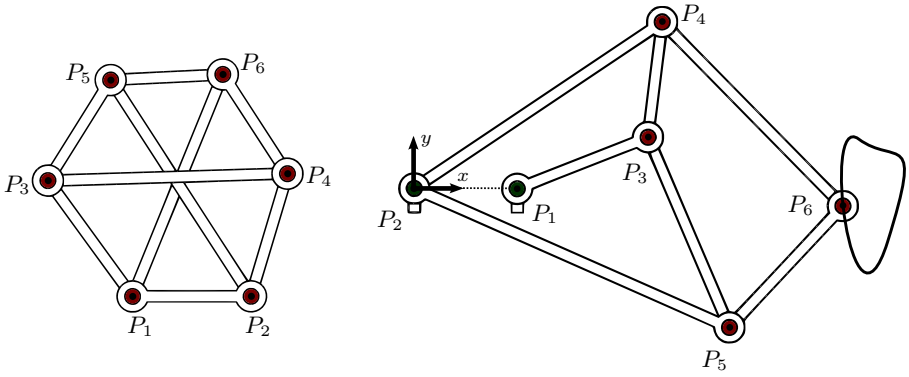

Figure 1: If the link connecting P_1 and P_6 is eliminated from the Dixon linkage **(left)**, and the location of P_1 and P_2 is fixed on the plane, the generalized Peaucellier linkage is obtained **(right)**.

obtain the generalized Peaucellier linkage in Fig. 1(right). As in the standard Peaucellier linkage, all non-fixed centers except P_6 trace circles. We will show how the coupler curve traced by P_6 can be derived from the closure polynomial of the Dixon linkage thus obtaining its general expression. To our knowledge, this general expression was previously unknown.

The rest of this paper is organized as follows. To make the presentation self-contained, Section 2 contains some basic mathematical background on Distance Geometry used in subsequent sections. Then, Section 3 presents a simple method to obtain the univariate closure polynomial for the Dixon linkage. Some particular cases, in which the degree of this polynomial drops, are studied in in Section 4 based on the analysis of the cases in which some factors of the leading and independent coefficients of the polynomial vanish. Then, the obtained closure polynomial is used, in Section 5, for the derivation of the coupler curve equation of the generalized Peaucellier linkage. Finally, the main contributions and prospects for future research are summarized in Section 6.

2. Preliminaries

Given the point sequences $P_{i_1}, \ldots, P_{i_n}$, and $P_{j_1}, \ldots, P_{j_n}$, we define:

$$D(i_1, \ldots, i_n; j_1, \ldots, j_n) = \begin{vmatrix} 0 & 1 & \ldots & 1 \\ 1 & s_{i_1,j_1} & \ldots & s_{i_1,j_n} \\ \vdots & \vdots & \ddots & \vdots \\ 1 & s_{i_n,j_1} & \ldots & s_{i_n,j_n} \end{vmatrix},$$

and

$$E(i_1, \ldots, i_{n-1}; j_1, \ldots, j_n) = \begin{vmatrix} 1 & \ldots & 1 \\ s_{i_1,j_1} & \ldots & s_{i_1,j_n} \\ \vdots & \ddots & \vdots \\ s_{i_{n-1},j_1} & \ldots & s_{i_{n-1},j_n} \end{vmatrix}.$$

where $s_{p,q}$ stands for the squared distance between P_p and P_q. When the two point sequences are the same, it is convenient to abbreviate $D(i_1, \ldots, i_n; i_1, \ldots, i_n)$ by $D(i_1, \ldots, i_n)$.

For any four points in $\mathbb{E}^2$, say P_i, P_j, P_k and P_l, the following properties hold [8, pp. 737-738]:

Property 1: $D(i,j,k,l) = 0$.

Property 2: $D(i,j;k,l) = 0$ if, and only if, $|_{i,j}$ and $|_{k,l}$ are orthogonal.

Property 3: $D(i,j,k;i,j,l) = 16\,A_{i,j,k}A_{i,j,l}$, where $A_{m,n,o}$ denotes the oriented area of $\triangle_{m,n,o}$ defined as positive when the sequence of points P_m, P_n, and P_o is traversed clockwise and negative otherwise. As a consequence, $D(i,j,k) = 16\,A_{i,j,k}^2$.

By expanding the determinants in $D(i,j,k;i,j,l) = 16\,A_{i,j,k}A_{i,j,l}$ and $D(i,j,k) = 16\,A_{i,j,k}^2$, it is possible to conclude that

$$s_{k,l} = \frac{1}{2\,s_{i,j}}\big[s_{j,k}(s_{i,j}+s_{i,l}-s_{j,l}) - s_{i,k}(-s_{i,j}+s_{i,l}-s_{j,l}) - s_{i,j}(s_{i,j}-s_{i,l}-s_{j,l}) + 16\,A_{i,j,k}A_{i,j,l}\big], \tag{1}$$

and

$$A_{i,j,k} = \pm\frac{1}{4}\sqrt{(s_{i,j}+s_{i,k}+s_{j,k})^2 - 2\,(s_{i,j}^2+s_{i,k}^2+s_{j,k}^2)}, \tag{2}$$

respectively. Both expressions will be useful later.

For any five points in $\mathbb{E}^2$, say P_i, P_j, P_k, P_l, and P_m, the following property also holds [9]:

Property 4: $E(j,l;i,k,m) = 0$ if, and only if, the center of the circle defined by P_i, P_k, and P_m is on the line defined by P_j and P_l.

A *dyad*, $\wedge_{i,j,k}$, consists of two segments, $|_{i,j}$ and $|_{j,k}$, connected through P_j. Two dyads can be connected by their end-points to form a quadrilateral. For example, the quadrilateral $\square_{i,j,k,l}$ with diagonals $|_{i,k}$ and $|_{j,l}$ can either be seen as formed by the set of dyads $\{\wedge_{i,j,k}, \wedge_{i,l,k}\}$ or $\{\wedge_{j,k,l}, \wedge_{j,i,l}\}$. Finally, three dyads connected by their end-points, say $\wedge_{j,k,l}$, $\wedge_{j,i,l}$, and $\wedge_{j,m,l}$, will be denoted by $\diamondsuit_{j,k,i,m,l}$.

Now, let us constrain the lengths of the edges of $\square_{i,j,k,l}$ as follows:

$$\left.\begin{array}{l} s_{l,i} = s_{j,i} + \lambda \\ s_{l,k} = s_{j,k} + \lambda \end{array}\right\} \tag{3}$$

which is always possible provided that the above system has a solution for λ. That is, if, and only if,

$$D(j,l;i,k) = \begin{vmatrix} s_{j,i}-s_{l,i} & 1 \\ s_{j,k}-s_{l,k} & 1 \end{vmatrix} = \begin{vmatrix} 0 & 1 & 1 \\ 1 & s_{j,i} & s_{j,k} \\ 1 & s_{l,i} & s_{l,k} \end{vmatrix} = 0. \tag{4}$$

In other words, if $\square_{i,j,k,l}$ satisfies (3), its diagonals are orthogonal according to Property 2. In this case $\square_{i,j,k,l}$ is called *orthodiagonal*.

Finally, let us constrain the lengths of the edges of $\diamondsuit_{j,k,i,m,l}$ as follows:

$$\left.\begin{array}{l} s_{j,m} = \mu s_{j,i} + (1-\mu)s_{j,k} \\ s_{l,m} = \mu s_{l,i} + (1-\mu)s_{l,k} \end{array}\right\} \tag{5}$$

which is always possible provided that the above system has a solution for μ. That is, if, and only if,

$$E(j,l;i,k,m) = \begin{vmatrix} s_{j,i} - s_{j,k} & s_{j,k} - s_{j,m} \\ s_{l,i} - s_{l,k} & s_{l,k} - s_{l,m} \end{vmatrix} = \begin{vmatrix} 1 & 1 & 1 \\ s_{j,i} & s_{j,k} & s_{j,m} \\ s_{l,i} & s_{l,k} & s_{l,m} \end{vmatrix} = 0. \tag{6}$$

In other words, if $\diamondsuit_{j,k,i,m,l}$ satisfies (5), then P_k, P_i, and P_m define a circle whose center is on the line defined by P_j and P_l according to Property 4. In this case, $\diamondsuit_{j,k,i,m,l}$ will be called a *diamond*.

3. Position analysis of the Dixon linkage

The six joint centers $P_1, \ldots, P_6$ of the Dixon linkage in Fig. 1 define the nine quadrilaterals $\square_{2,1,6,5}$, $\square_{1,2,4,3}$, $\square_{1,2,5,3}$, $\square_{2,1,6,4}$, $\square_{1,3,4,6}$, $\square_{1,3,5,6}$, $\square_{2,4,6,5}$, $\square_{2,4,3,5}$, and $\square_{3,4,6,5}$. Any of the six unknown distances ($s_{1,4}$, $s_{4,5}$, $s_{5,1}$, $s_{2,3}$, $s_{3,6}$, and $s_{6,2}$) in this linkage corresponds to the length of one diagonal of three of these nine quadrilaterals. For example, $|_{2,6}$ is a diagonal of $\square_{2,1,6,4}$, $\square_{2,1,6,5}$, and $\square_{2,4,6,5}$. Then, using Property 3 and equation (1),

$$D(2,6,1;2,6,4) = 16\, A_{2,6,1} A_{2,6,4} \implies s_{1,4} = f_1(s_{2,6}) \tag{7}$$

$$D(2,6,1;2,6,5) = 16\, A_{2,6,1} A_{2,6,5} \implies s_{1,5} = f_2(s_{2,6}) \tag{8}$$

$$D(2,6,4;2,6,5) = 16\, A_{2,6,4} A_{2,6,5} \implies s_{4,5} = f_3(s_{2,6}) \tag{9}$$

Moreover, using Property 1,

$$D(1,3,4,5) = 0 \implies f_4(s_{1,4}, s_{1,5}, s_{4,5}) = 0. \tag{10}$$

Now, by replacing (7), (8), and (9) in (10) and rearranging terms, we obtain:

$$\Phi_1 + \Phi_2 A_{2,6,1}\, A_{2,6,4} + \Phi_3 A_{2,6,1}\, A_{2,6,5} + \Phi_4 A_{2,6,4}\, A_{2,6,5} = 0, \tag{11}$$

where Φ_1, Φ_2, Φ_3, and Φ_4 are polynomials in $s_{2,6}$. Therefore, (11) is a scalar equation in a single unknown, $s_{2,6}$, whose roots determine the assembly modes of the Dixon linkage. Indeed, for each of these roots, given the position vectors $\mathbf{p}_1$ and $\mathbf{p}_2$, we can determine the position of the remaining four joints of the linkage by computing, for instance, the following sequence of bilaterations (see [6] for details): computing $\mathbf{p}_6$ from $\mathbf{p}_1$ and $\mathbf{p}_2$, then $\mathbf{p}_4$ from $\mathbf{p}_2$ and $\mathbf{p}_6$, then $\mathbf{p}_5$ from $\mathbf{p}_2$ and $\mathbf{p}_6$, and finally $\mathbf{p}_3$ from $\mathbf{p}_4$ and $\mathbf{p}_5$. This leads to up to 32 locations for P_3. Those locations that satisfy the distance imposed by the binary link connecting P_3 and P_1 correspond to the valid assembly modes.

In order to transform (11) into a polynomial, it is possible to clear all square roots associated with $A_{2,6,1}$, $A_{2,6,4}$, and $A_{2,6,5}$ (see equation (2)) by iteratively isolating some terms and squaring both sides of the resulting equation. This process yields the distance-based univariate closure equation of the Dixon linkage in polynomial form

$$\begin{aligned} &- 2\,\Phi_1^2\Phi_2^2 A_{2,6,1}^2 A_{2,6,4}^2 - 2\,\Phi_1^2\Phi_3^2 A_{2,6,1}^2 A_{2,6,5}^2 - 2\,\Phi_1^2\Phi_4^2 A_{2,6,4}^2 A_{2,6,5}^2 \\ &+ 8\,\Phi_1\Phi_2 A_{2,6,1}^2 A_{2,6,4}^2 \Phi_3 A_{2,6,5}^2 \Phi_4 + \Phi_2^4 A_{2,6,1}^4 A_{2,6,4}^4 + \Phi_4^4 A_{2,6,4}^4 A_{2,6,5}^4 \\ &+ \Phi_3^4 A_{2,6,1}^4 A_{2,6,5}^4 - 2\,{\Phi_2}^2 A_{2,6,1}^4 A_{2,6,4}^2 \Phi_3^2 A_{2,6,5}^2 - 2\,\Phi_2^2 A_{2,6,1}^2 A_{2,6,4}^4 \Phi_4^2 A_{2,6,5}^2 \\ &- 2\,\Phi_3^2 A_{2,6,1}^2 A_{2,6,5}^4 \Phi_4^2 A_{2,6,4}^2 + \Phi_1^4 = 0, \end{aligned} \tag{12}$$

which, when fully expanded, leads to the octic polynomial equation

$$\sum_{n=0}^{8} C_n \, s_{2,6}^n = 0. \tag{13}$$

The coefficients C_i, $i = 1, \ldots, 8$, are polynomials in the nine link lengths $s_{1,2}$, $s_{1,3}$, $s_{1,6}$, $s_{2,4}$, $s_{2,5}$, $s_{3,4}$, $s_{3,5}$, $s_{4,6}$, and $s_{5,6}$. They can be expressed as:

$$\begin{aligned}
C_8 &= 768\, s_{3,5}\, s_{1,3}^2\, s_{5,6}^3\, s_{2,4}\, s_{3,4}\, s_{2,5}^2 + 1536\, s_{3,5}\, s_{1,3}^2\, s_{5,6}^2\, s_{2,4}\, s_{3,4}\, s_{2,5}^3 - 512\, s_{3,5}\, s_{1,3}^3\, s_{5,6}^3 + \ldots, \\
C_7 &= -1536\, s_{1,3}^4\, s_{4,6}^3\, s_{2,5}^2\, s_{3,5}^2 + 2816\, s_{1,3}^5\, s_{4,6}^2\, s_{2,5}^2\, s_{3,5}^2 - 1024\, s_{1,3}^3\, s_{4,6}^2\, s_{2,5}^3\, s_{1,6}^3 + \ldots, \\
C_6 &= -512\, s_{1,3}^6\, s_{2,4}^2\, s_{5,6}^4 - 256\, s_{3,5}^6\, s_{1,6}^4\, s_{1,2}^2 + 512\, s_{3,5}^6\, s_{1,2}^3\, s_{1,6}^3 + \ldots, \\
C_5 &= -512 s_{3,5}^8 s_{4,6}^3 s_{1,2}^2 - 1024 s_{3,4}^5 s_{1,2}^3 s_{5,6}^5 + 1536 s_{3,5}^7 s_{1,2}^3 s_{4,6}^3 + \ldots, \\
C_4 &= 256\, s_{3,5}^4\, s_{2,4}^5\, s_{1,6}^5 - 3584\, s_{4,6}\, s_{5,6}^3\, s_{1,2}^5\, s_{3,5}^4\, s_{3,4} - 24064\, s_{4,6}^3\, s_{5,6}^3\, s_{2,5}^2\, s_{3,5}^2\, s_{1,2}^4 + \ldots, \\
C_3 &= -768\, s_{3,5}^5\, s_{1,6}^4\, s_{2,4}^6 + 512\, s_{3,4}^7\, s_{1,2}^3\, s_{5,6}^5 + 512\, s_{3,4}^7\, s_{1,2}^5\, s_{5,6}^3 + \ldots, \\
C_2 &= -256\, s_{3,5}^3\, s_{1,6}^2\, s_{2,4}^6\, s_{3,4}^2\, s_{2,5}^3 - 3072\, s_{1,2}^2\, s_{4,6}^4\, s_{2,5}^5\, s_{2,4}^3\, s_{5,6}^2 + \ldots, \\
C_1 &= -512\, s_{1,3}^4\, s_{1,2}^2\, s_{2,5}^7\, s_{4,6}^2\, s_{5,6}\, s_{2,4} - 256\, s_{1,3}^5\, s_{4,6}^6\, s_{2,5}\, s_{5,6}^3\, s_{3,5}\, s_{1,6} + \ldots, \\
C_0 &= 512\, s_{1,6}\, s_{3,5}^2\, s_{1,2}^5\, s_{2,4}^4\, s_{3,4}^2\, s_{2,5}^3\, s_{1,3} - 3840\, s_{1,6}^3\, s_{1,3}^4\, s_{4,6}^4\, s_{5,6}^3\, s_{2,4}^3\, s_{3,5} + 5120\, s_{1,6}^3\, s_{1,3}^4 + \ldots.
\end{aligned}$$

The full expressions for these coefficients cannot be included here due to space limitations. Actually, $C_0, \ldots, C_8$ consist of 127.924, 178.530, 198.984, 183.532, 141.597, 93.264, 55.483, 27.666, and 11.070 monomials, respectively. However, they can be easily reproduced using a computer algebra system following the steps given above.

As an example, let us set $s_{1,2} = 13689/100$, $s_{1,3} = 89$, $s_{1,6} = 80$, $s_{2,4} = (\sqrt{85}+1)^2$, $s_{2,5} = 85$, $s_{3,4} = 241$, $s_{3,5} = 137$, $s_{4,6} = 122$, and $s_{5,6} = 1521/25$. Then, by replacing these link lengths in the closure polynomial derived above, we obtain:

$$\begin{aligned}
&3.9377\,10^{21}\, s_{2,6}^8 - 2.8046\,10^{24}\, s_{2,6}^7 + 6.7900\,10^{26}\, s_{2,6}^6 - 6.7652\,10^{28}\, s_{2,6}^5 + 3.3732\,10^{30}\, s_{2,6}^4 \\
&- 9.0927\,10^{31}\, s_{2,6}^3 + 1.3290\,10^{33}\, s_{2,6}^2 - 9.7683\,10^{33}\, s_{2,6} + 2.7761\,10^{34}.
\end{aligned} \tag{14}$$

This polynomial has 8 real roots. The resulting assembly modes, one each for the 8 real roots, for the case in which $\mathbf{p}_1 = (0,0)^T$ and $\mathbf{p}_2 = (\frac{117}{10}, 0)^T$ are shown in Fig. 2. Mirror configurations with respect to the x-axis are not considered as different assembly modes. This example was already used by Walter and Husty in [5]. It can be verified that the results obtained here are in agreement with those reported by these authors.

4. Special cases of the Dixon linkage

The Dixon linkage in Fig. 1 contains:

1. Nine quadrilaterals, namely, $\square_{2,1,6,5}$, $\square_{1,2,4,3}$, $\square_{1,2,5,3}$, $\square_{2,1,6,4}$, $\square_{1,3,4,6}$, $\square_{1,3,5,6}$, $\square_{2,4,6,5}$, $\square_{2,4,3,5}$, and $\square_{3,4,6,5}$. If, for example, $\square_{2,1,6,5}$ is orthodiagonal, then $D(2,6;1,5) = 0$. Likewise for all other quadrilaterals.
2. Six sets of three dyads sharing their end-points, namely, $\diamondsuit_{1,3,6,2,5}$, $\diamondsuit_{3,5,4,1,6}$, $\diamondsuit_{5,6,2,3,4}$, $\diamondsuit_{6,4,1,5,2}$, $\diamondsuit_{4,2,3,6,1}$, and $\diamondsuit_{2,1,5,4,3}$. If, for example, $\diamondsuit_{1,3,6,2,5}$ is a diamond, then $E(1,5;2,3,6) = 0$. Likewise for all other sets of three dyads.

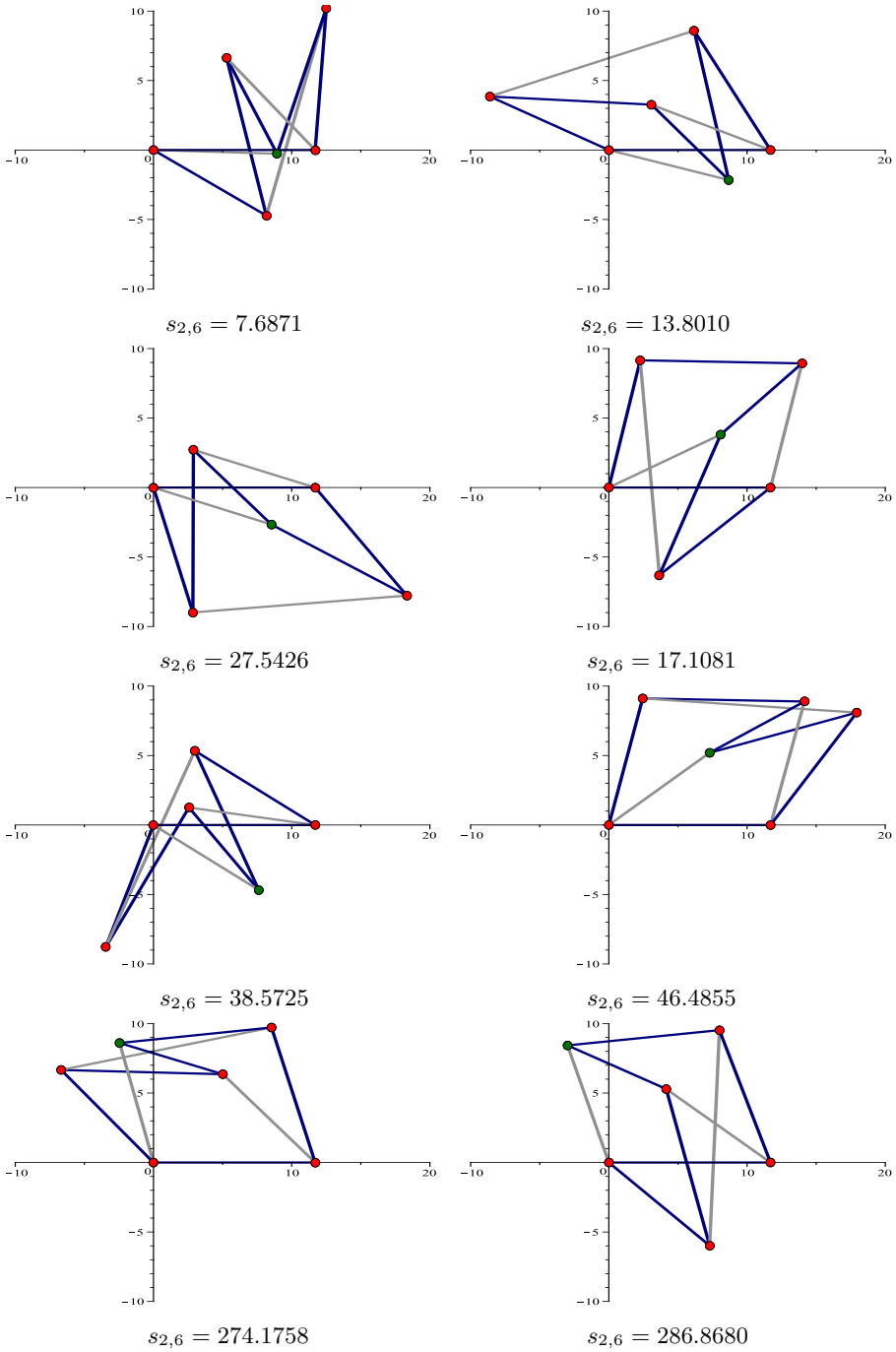

Figure 2: A Dixon linkage with eight assembly modes. According to Fig. 1, the blue lines correspond to the links defining the hexagon, and the gray lines to the three diagonals. P_1 is located at the origin, and P_2 is on the $x-$axis.

A remarkable result arises when observing that the leading and independent coefficients in (13) can be factored as follows:

$$C_8 = 256\, D(1,4;2,3)D(1,5;2,3)D(1,4;3,6)D(1,5;3,6)D(2,3;4,5) \\ D(3,6;4,5)E(3,6;1,4,5)E(2,3;1,4,5), \tag{15}$$

$$C_0 = 256\, C_x\, D(2,6;1,5)D(2,6;1,4)D(2,6;4,5) \\ E(4,5;2,3,6)E(1,5;2,3,6)E(1,4;2,3,6), \tag{16}$$

where C_x is a factor, apparently related to $E(2,6;1,4,5)$, whose geometric interpretation remains elusive.

Clearly, when any of above factors vanish, the number of assembly modes drops. Thanks to Property 2 and 4, the geometric conditions for this to happen are expressible in terms of the presence of orthodiagonal quadrilaterals and diamonds. Several cases are exemplified below.

4.1. Orthodiagonal quadrilaterals and no diamonds

If we impose the constraints

$$s_{2,4} = s_{3,5},\ s_{3,4} = 2\, s_{3,5} - s_{2,5}, \tag{17}$$

then $\square_{2,4,3,5}$ is orthodiagonal. In this case, the closure polynomial reduces to a polynomial of 7th-degree with leading coefficient

$$256\, (s_{2,5} - s_{3,5})^2\, (s_{2,5} - s_{5,6} + s_{4,6} - s_{3,5})\, (s_{5,6} + s_{1,3} - s_{1,6} - s_{3,5}) \\ (s_{4,6} + s_{1,3} + s_{2,5} - s_{1,6} - 2\, s_{3,5})\, (s_{1,3}s_{4,6} - s_{1,3}s_{5,6} - s_{3,5}s_{1,6} + s_{1,6}s_{2,5} - s_{2,5}s_{5,6} \\ - s_{3,5}s_{4,6} + 2\, s_{3,5}s_{5,6})\, (-s_{1,3} + s_{4,6} + s_{1,2} - s_{5,6})\, (s_{1,2} - s_{1,3} - s_{2,5} + s_{3,5})^3 .$$

Since the polynomial degree of this special case is odd, it is not possible to have an instance with all the assembly modes real [10]. If we also impose the constraints

$$s_{1,3} = s_{4,6} = s_{3,5},\ s_{1,6} = s_{2,5}, \tag{18}$$

then $\square_{1,3,4,6}$ is also orthodiagonal, and the closure polynomial reduces to a sextic with leading coefficient

$$256\, (s_{2,5} - s_{5,6})^3\, (s_{2,5} - s_{3,5})^4\, (s_{1,2} - s_{5,6})^2\, (s_{1,2} - s_{2,5})^3 .$$

If we also impose the constraint $s_{1,2} = s_{5,6}$, $\square_{2,4,3,5}$ and $\square_{1,3,4,6}$ remain as the only orthodiagonal quadrilaterals, and still no diamonds arise. Now, the closure polynomial reduces to a quartic. If, in addition, we set

$$s_{1,2} = s_{5,6} = a = \pm \frac{-s_{2,5}^2 - 4\, s_{3,5}^2 + 4\, s_{3,5}s_{2,5} + 2\sqrt{s_{2,5}(2\, s_{3,5} - s_{2,5})(s_{2,5} - s_{3,5})^2}}{s_{2,5} - 2\, s_{3,5}}, \tag{19}$$

such quartic simplifies to the biquadratic

$$D_4 s_{2,6}^4 + D_2 s_{2,6}^2 + D_0, \tag{20}$$

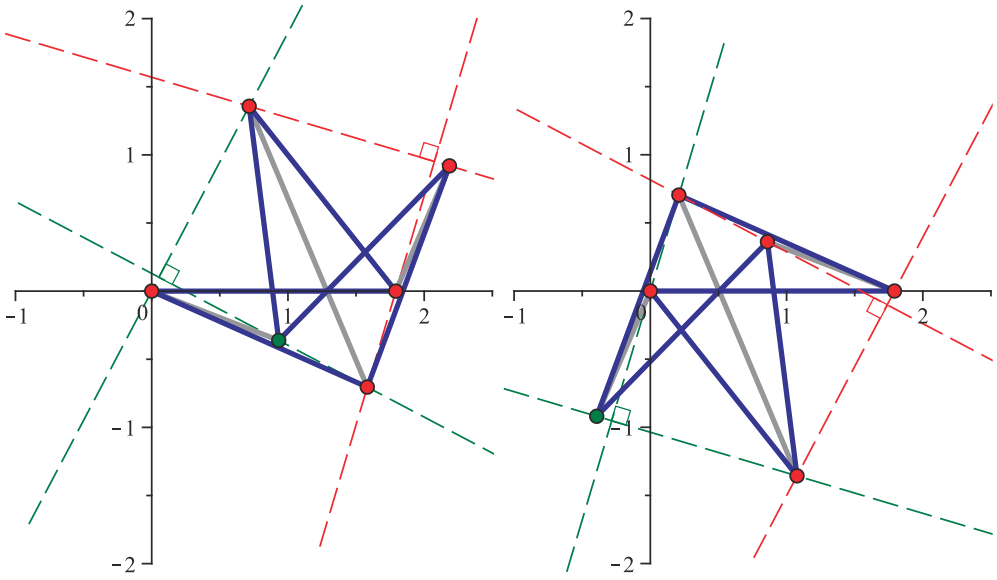

$$s_{2,6} = \sqrt{\tfrac{224}{5} - \tfrac{64}{5}\sqrt{5} - \tfrac{32}{5}\sqrt{55 - 22\sqrt{5}}} \qquad s_{2,6} = \sqrt{\tfrac{224}{5} - \tfrac{64}{5}\sqrt{5} + \tfrac{32}{5}\sqrt{55 - 22\sqrt{5}}}$$

Figure 3: The two assembly modes of a Dixon linkage satisfying the constraints (17), (18), and (19). This linkage contains two orthodiagonal quadrilaterals, $\square_{2,4,3,5}$ and $\square_{1,3,4,6}$, whose diagonals are represented in red and green, respectively.

where

$$\begin{aligned}
D_4 =&(s_{2,5}-s_{3,5})^2,\\
D_2 =&(2\,s_{2,5}-4\,s_{3,5})\,a^3+(18\,s_{3,5}^2-16\,s_{3,5}\,s_{2,5}+4\,s_{2,5}^2)\,a^2\\
&+(44\,s_{3,5}^2\,s_{2,5}+2\,s_{2,5}^3-32\,s_{3,5}^3-20\,s_{3,5}\,s_{2,5}^2)\,a\\
&-24\,s_{3,5}\,s_{2,5}^3-32\,s_{3,5}^3\,s_{2,5}+34\,s_{3,5}^2\,s_{2,5}^2+8\,s_{2,5}^4+16\,s_{3,5}^4,\\
D_0 =&(s_{2,5}-s_{3,5})^2(a-s_{2,5})^4.
\end{aligned}$$

As an example, let us set $s_{1,2}=5-(4/5)\sqrt{5}$, $s_{1,3}=3$, $s_{1,6}=1$, $s_{2,4}=3$, $s_{2,5}=1$, $s_{3,4}=5$, $s_{3,5}=3$, $s_{4,6}=3$, and $s_{5,6}=5-(4/5)\sqrt{5}$. It can be verified that these link lengths satisfy the constraints (17), (18), and (19). Then, by replacing these values in (20), we obtain

$$4\,s_{2,6}^4+\left(-\frac{1792}{5}+\frac{512}{5}\sqrt{5}\right)s_{2,6}^2-\frac{24576}{25}\sqrt{5}+\frac{57344}{25}, \tag{21}$$

whose two positive roots are $s_{2,6}=+\sqrt{\frac{224}{5}-\frac{64}{5}\sqrt{5}\pm\frac{32}{5}\sqrt{55-22\sqrt{5}}}$. The resulting two real assembly modes, for the case in which $\mathbf{p}_1=(0,0)^T$ and $\mathbf{p}_2=(1/5\sqrt{125-20\sqrt{5}},0)^T$, appear in Fig. 3. The diagonals of the orthodiagonal quadrilaterals $\square_{2,4,3,5}$ and $\square_{1,3,4,6}$ are represented in red and green, respectively. Remember that mirror configurations with respect to the x-axis are not considered as different assembly modes.

4.2. Diamonds and no orthodiagonal quadrilaterals

If we would impose the constraint

$$s_{4,6}=s_{5,6}=s_{1,6}, \tag{22}$$

then $\diamondsuit_{3,5,4,1,6}$ and $\diamondsuit_{2,5,1,4,6}$ would be diamonds, and the closure polynomial would reduce to a 7th-degree polynomial. Likewise, if we would impose the constraints

$$s_{1,2}=\lambda\,s_{1,3},\ \ s_{2,4}=\lambda\,s_{3,4},\ \ s_{2,5}=\lambda\,s_{3,5}, \tag{23}$$

with $\lambda\neq 0,1$, $\diamondsuit_{2,1,4,5,3}$ would be a diamond (observe that if $\lambda=1$, $\square_{2,1,3,4}$, $\square_{2,1,3,5}$, and $\square_{2,4,3,5}$ would be, in addition, orthodiagonal).

If the constraints in (22) and (23) are simultaneously satisfied, the closure polynomial reduces to

$$256\,\lambda^4 s_{1,6}^2\,(s_{3,4}-s_{3,5})^4\,(s_{1,3}-s_{3,5})^4\,(s_{1,3}-s_{3,4})^4\,(\lambda-1)^4\,(\lambda\,s_{1,6}-s_{2,6})^4\,, \tag{24}$$

which has a single root, $s_{2,6}=\lambda\,s_{1,6}$, of multiplicity 4. As an example, let us set $s_{1,2}=3$, $s_{1,3}=1$, $s_{1,6}=3/2$, $s_{2,4}=6$, $s_{2,5}=15/2$, $s_{3,4}=2$, $s_{3,5}=5/2$, $s_{4,6}=3/2$, and $s_{5,6}=3/2$. By replacing these values in (24), we obtain the polynomial

$$\frac{59049}{4}\,(2\,s_{2,6}-9)^4\,, \tag{25}$$

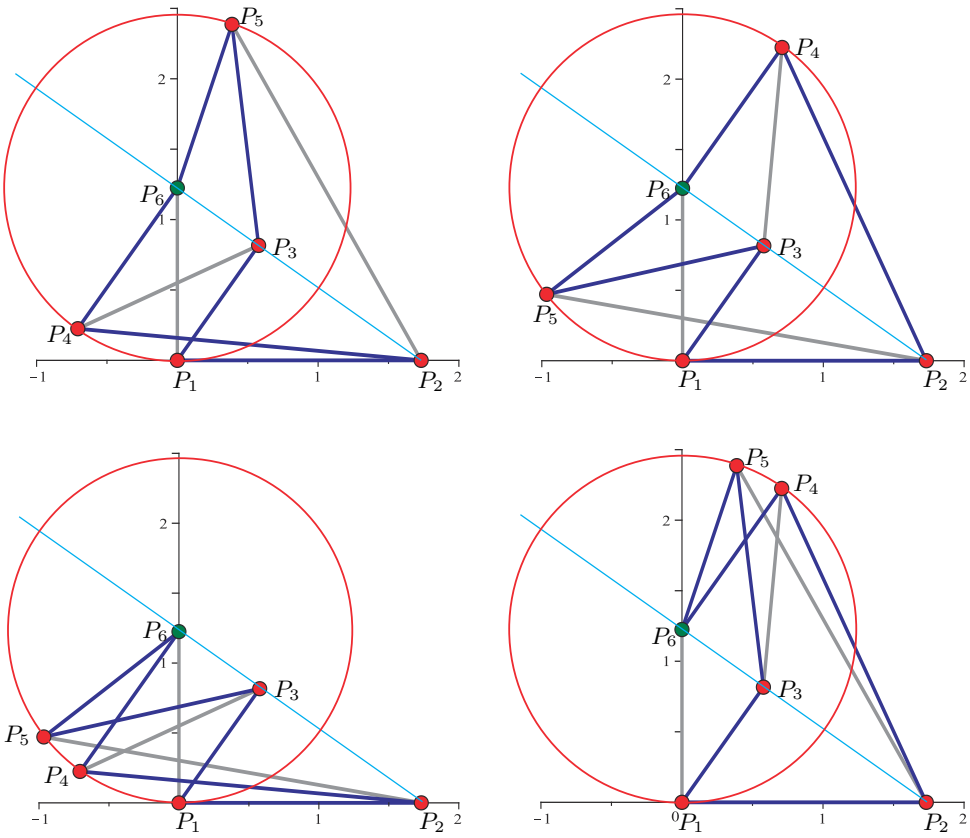

Figure 4: The four assembly modes of a Dixon linkage satisfying the constraints (22) and (23). In this case, the general closure polynomial reduces to a quartic with a single root of multiplicity 4.

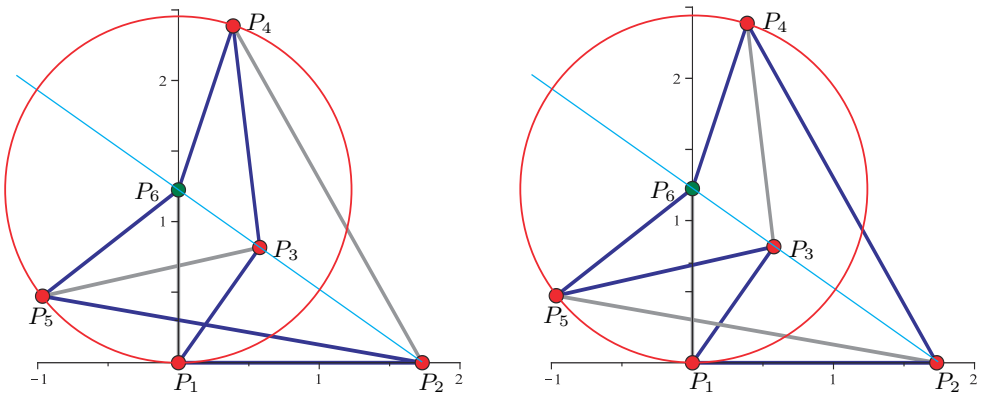

Figure 5: The two rigid assembly modes of a Dixon linkage satisfying the constraints (26) and (27). In this case, the linkage also has a movable assembly mode.

whose root at $s_{2,6} = 9/2$ with multiplicity 4 leads to the four assembly modes shown in Fig. 4 for the case in which $\mathbf{p}_1 = (0,0)^T$ and $\mathbf{p}_2 = (\sqrt{3},0)^T$.

Let us analyze the obtained result geometrically. Since $\diamondsuit_{2,1,4,5,3}$ is a diamond, the center of the circle defined by P_1, P_4, and P_5 is on the line defined by P_2 and P_3. Moreover, since P_6 is at the same distance of P_1, P_4, and P_5, it is necessarily the center of this circle (shown in red in Fig. 4). As a consequence, P_2, P_3, and P_6 are on a line (shown in light blue in Fig. 4). Now, take any of the four assembly modes in Fig. 4 and observe how the sets of three links connected to P_1, P_4, and P_5 can flip over the line defined by P_2, P_3, and P_6 without violating any distance constraint. This permits generating 7 other valid assembly modes corresponding, up to mirror reflections, to the other three assembly modes shown in Fig. 4. Now, one interesting question arises: what would happen if, in any of these assembly modes, P_1, P_4 or P_5 would coincide? This situation is analyzed in the next subsection.

4.3. Orthodiagonal quadrilaterals and diamonds

If we impose the constraints

$$s_{2,4} = s_{2,5},\ \ s_{3,4} = s_{3,5}, \tag{26}$$

then $\square_{2,4,3,5}$ is orthodiagonal and $\diamondsuit_{2,1,4,5,3}$ is a diamond. In this case, the general closure polynomial reduces to a polynomial of 6th-degree. If we also impose the constraint

$$s_{4,6} = s_{5,6}, \tag{27}$$

then, in addition, $\square_{3,4,6,5}$ and $\square_{2,4,6,5}$ are orthodiagonal, and $\diamondsuit_{3,5,4,1,6}$ and $\diamondsuit_{5,6,2,3,4}$, diamonds. In this case, the general closure polynomial reduces to

$$(\gamma_1\, s_{2,6} + \gamma_0)^2, \tag{28}$$

where

$$\begin{aligned}\gamma_1 =& (s_{5,6}-s_{3,5}-s_{1,6}+s_{1,3})(s_{3,5}-s_{1,3}-s_{2,5}+s_{1,2}),\\ \gamma_0 =& (s_{5,6}-s_{2,5}+s_{1,2}-s_{1,6})(s_{3,5}s_{1,2}-s_{1,2}s_{5,6}+s_{1,3}s_{5,6}+s_{1,6}s_{2,5}-s_{1,3}s_{2,5}-s_{3,5}s_{1,6}).\end{aligned}$$

In this case, it is interesting to realize that the link lengths of the three links connected to P_1 can be independently selected without violating the constraints given in (26) and (27). Thus, this linkage could be used as the basis for a planar positioning robot with three degrees of freedom and simple forward kinematics. As an example, let us set $s_{1,2} = 3$, $s_{1,3} = 1$, $s_{1,6} = 3/2$, $s_{2,4} = 15/2$, $s_{2,5} = 15/2$, $s_{3,4} = 5/2$, $s_{3,5} = 5/2$, $s_{4,6} = 3/2$, and $s_{5,6} = 3/2$. By replacing these link lengths in (28), we obtain the polynomial

$$\left(\frac{9}{2}\, s_{2,6} - \frac{81}{4}\right)^2, \tag{29}$$

whose double root at $s_{2,6} = 9/2$ leads to the two rigid configurations shown in Fig. 5 for the case in which $\mathbf{p}_1 = (0,0)^T$ and $\mathbf{p}_2 = (\sqrt{3},0)^T$.

Following a similar reasoning to the one used in the previous subsection, we conclude that the sets of three links connected to P_1, P_4, and P_5 can flip over the line defined by P_2, P_3, and P_6 without violating any distance constraint. In this case, P_4 and P_5 can coincide leading to an assembly mode with mobility 1. Actually, Ivory's theorem predicts this behavior [4].

Finally, it is worth mentioning that there are two very special cases of the Dixon linkage, known as the two Dixon's mechanisms [1, 3], that are continuously movable with mobility 1 with no rigid assembly modes and no coincident joint centers. These two mechanisms satisfy the following two sets of constraints:

$$\begin{aligned} &s_{4,6} + s_{3,5} = s_{5,6} + s_{3,4}, \;\; s_{1,6} + s_{3,5} = s_{1,3} + s_{5,6}, \\ &s_{2,4} + s_{3,5} = s_{2,5} + s_{3,4}, \;\; s_{1,2} + s_{3,5} = s_{1,3} + s_{2,5}, \end{aligned} \tag{30}$$

and

$$\begin{aligned} &s_{5,6} = s_{2,4}, \;\; s_{1,3} = s_{2,4}, \;\; s_{1,2} = s_{3,4}, \\ &s_{4,6} = s_{2,5}, \;\; s_{3,5} = s_{1,6}, \;\; s_{1,2} + s_{5,6} = s_{2,5} + s_{1,6}, \end{aligned} \tag{31}$$

respectively [5]. In the Dixon's mechanism satisfying (30), all the nine quadrilaterals in the linkage are orthogonal and all the six sets of three dyads sharing their end-points are diamonds. In the Dixon's mechanism satisfying (31), only $\square_{3,4,6,5}$ and $\square_{2,1,6,5}$ are orthogonal, and $\diamondsuit_{2,1,5,4,3}$ and $\diamondsuit_{4,2,3,6,1}$ are diamonds.

5. Position analysis of the generalized Peaucellier linkage

In this Section, we show how the closure polynomial for the Dixon linkage in Fig 1(left) can be used to obtain the curve traced by P_6 in Fig 1(right).

To slightly simplify the formulation, all link lengths can be normalized with respect to the length of the base link. Thus, without loss of generality, we can set $s_{1,2} = 1$. Therefore, if we set $\mathbf{p}_1 = (1,0)^T$, $\mathbf{p}_2 = (0,0)^T$, and $\mathbf{p}_6 = (x,y)^T$, we have that

$$s_{1,6} = (x-1)^2 + y^2, \tag{32}$$

$$s_{2,6} = x^2 + y^2. \tag{33}$$

Thus, to determine the curve traced by P_6, we just need to replace (32) and (33) in the closure equation of the Dixon linkage given in (13). The result can beautifully expressed as:

$$\begin{aligned}
&p_0\left(x^2+y^2\right)^{11}+p_1\left(x^2+y^2\right)^{10}+p_2\left(x^2+y^2\right)^{9}+p_3\left(x^2+y^2\right)^{8}+p_4\left(x^2+y^2\right)^{7}\\
&+p_5\left(x^2+y^2\right)^{6}+p_6\left(x^2+y^2\right)^{5}+p_7\left(x^2+y^2\right)^{4}+p_8\left(x^2+y^2\right)^{3}+p_9\left(x^2+y^2\right)^{2}\\
&+p_{10}\left(x^2+y^2\right)+q_{11}+q_{10}+q_9+q_8+q_7+q_6+q_5+q_4+q_3+q_2+q_1+q_0=0, \quad (34)
\end{aligned}$$

where

$$\begin{aligned}
p_0 &= \alpha_0\\
p_1 &= \alpha_1\, x\\
p_2 &= \alpha_2\, x^2+\alpha_3\, y^2\\
p_3 &= \alpha_4\, x^3+\alpha_5\, x\, y^2\\
p_4 &= \alpha_6\, x^4+\alpha_7\, x^2\, y^2+\alpha_8\, y^4\\
p_5 &= \alpha_9\, x^5+\alpha_{10}\, x^3\, y^2+\alpha_{11}\, x\, y^4\\
p_6 &= \alpha_{12}\, x^6+\alpha_{13}\, x^4\, y^2+\alpha_{14}\, x^2\, y^4+\alpha_{15}\, y^6\\
p_7 &= \alpha_{16}\, x^7+\alpha_{17}\, x^5\, y^2+\alpha_{18}\, x^3\, y^4+\alpha_{19}\, x\, y^6\\
p_8 &= \alpha_{20}\, x^8+\alpha_{21}\, x^6\, y^2+\alpha_{22}\, x^4\, y^4+\alpha_{23}\, x^2\, y^6+\alpha_{24}\, y^8\\
p_9 &= \alpha_{25}\, x^9+\alpha_{26}\, x^7\, y^2+\alpha_{27}\, x^5\, y^4+\alpha_{28}\, x^3\, y^6+\alpha_{29}\, x\, y^8\\
p_{10} &= \alpha_{30}\, x^{10}+\alpha_{31}\, x^8\, y^2+\alpha_{32}\, x^6\, y^4+\alpha_{33}\, x^4\, y^6+\alpha_{34}\, x^2\, y^8+\alpha_{35}\, y^{10}\\
q_{11} &= \alpha_{36}\, x^{11}+\alpha_{37}\, x^9\, y^2+\alpha_{38}\, x^7\, y^4+\alpha_{39}\, x^5\, y^6+\alpha_{40}\, x^3\, y^8+\alpha_{41}\, x\, y^{10}\\
q_{10} &= \alpha_{42}\, x^{10}+\alpha_{43}\, x^8\, y^2+\alpha_{44}\, x^6\, y^4+\alpha_{45}\, x^4\, y^6+\alpha_{46}\, x^2\, y^8+\alpha_{47}\, y^{10}\\
q_9 &= \alpha_{48}\, x^9+\alpha_{49}\, x^7\, y^2+\alpha_{50}\, x^5\, y^4+\alpha_{51}\, x^3\, y^6+\alpha_{52}\, x\, y^8\\
q_8 &= \alpha_{53}\, x^8+\alpha_{54}\, x^6\, y^2+\alpha_{55}\, x^4\, y^4+\alpha_{56}\, x^2\, y^6+\alpha_{57}\, y^8\\
q_7 &= \alpha_{58}\, x^7+\alpha_{59}\, x^5\, y^2+\alpha_{60}\, x^3\, y^4+\alpha_{61}\, x\, y^6\\
q_6 &= \alpha_{62}\, x^6+\alpha_{63}\, x^4\, y^2+\alpha_{64}\, x^2\, y^4+\alpha_{65}\, y^6\\
q_5 &= \alpha_{66}\, x^5+\alpha_{67}\, x^3\, y^2+\alpha_{68}\, x\, y^4\\
q_4 &= \alpha_{69}\, x^4+\alpha_{70}\, x^2\, y^2+\alpha_{71}\, y^4\\
q_3 &= \alpha_{72}\, x^3+\alpha_{73}\, x\, y^2\\
q_2 &= \alpha_{74}\, x^2+\alpha_{75}\, y^2\\
q_1 &= \alpha_{76}\, x\\
q_0 &= \alpha_{77}
\end{aligned}$$

where α_i, $i = 0 \ldots 77$, are polynomials in $s_{1,3}$, $s_{2,4}$, $s_{2,5}$, $s_{3,4}$, $s_{3,5}$, $s_{4,6}$, and $s_{5,6}$. The expressions of all these coefficients cannot be included here due to space limitations, but they can be reproduced using a computer algebra system without much effort. Equation (34) corresponds to a 11-circular curve of degree 22 [11, pp. 87].

As an example, let us set $s_{1,3} = 9/2$, $s_{2,4} = 45/4$, $s_{2,5} = 109/4$, $s_{3,4} = 13/4$, $s_{3,5} = 25/4$, $s_{4,6} = 13/2$, and $s_{5,6} = 5$. Remember that all link lengths are assumed

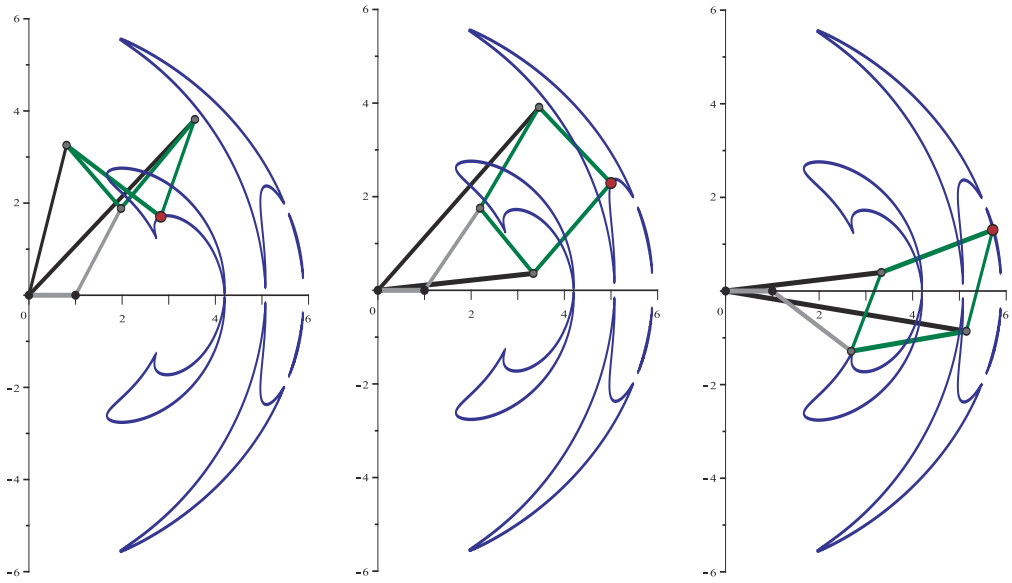

Figure 6: Example of a generalized Peaucellier linkage represented in three different configurations. The curve in blue represents the 11-circular coupler curve traced by P_6. $\square_{3,6,4,5}$ is represented in green, $\wedge_{5,2,4}$ in black, and $\wedge_{2,1,3}$ in gray.

to be normalized with respect to $s_{1,2}$. Hence, $s_{1,2} = 1$. By replacing these values in (34), we obtain the equation

$$
\begin{aligned}
&4769856\,(x^2+y^2)^{11} + 154321440\,x\,(x^2+y^2)^{10} + 4\,(77025433\,x^2 - 147788975\,y^2)\,(x^2\\
&+y^2)^9 - 24\,(1303744447\,x^3 + 1110046215\,x\,y^2)\,(x^2+y^2)^8 - 4\,(37412647751\,x^4\\
&+28949616460\,x^2\,y^2 - 5476551067\,y^4)\,(x^2+y^2)^7 + 2\,(1532684101319\,x^5\\
&+2576822045150\,x^3\,y^2 + 1075751046807\,x\,y^4)\,(x^2+y^2)^6 + \frac{1}{2}\,(24483722504627\,x^6\\
&+46893194350141\,x^4\,y^2 + 22378081433601\,x^2\,y^4 + 66265488247\,y^6)\,(x^2+y^2)^5\\
&-2\,(92557658056081\,x^7 + 236941009972511\,x^5\,y^2 + 199886755232779\,x^3\,y^4\\
&+55475448116349\,x\,y^6)\,(x^2+y^2)^4 + \ldots + \Big(-\frac{21369647416854306832493}{8192}\,x^2\\
&+\frac{19150328181751022802847}{8192}\,y^2\Big) - \frac{16960444285050329617435}{8192}\,x\\
&+\frac{48083411621190921235225}{65536} = 0.
\end{aligned}
\tag{35}
$$

Figure 6 shows this generalized Peaucellier linkage in three different configurations overlaping the curve traced by P_6.

Now, we can analyze an important particular case. Let us impose the constraints

$$
s_{2,4} = s_{2,5} \text{ and } s_{4,6} = s_{5,6}. \tag{36}
$$

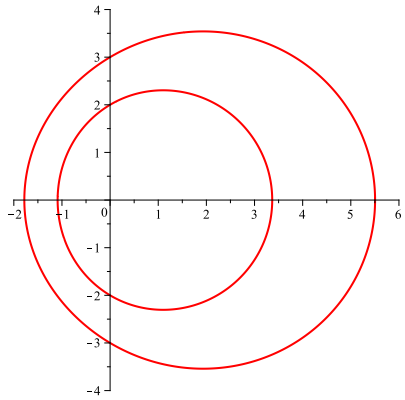

$s_{1,3}$=$s_{2,5}$=2, $s_{3,5}$=4, $s_{5,6}$ = 8

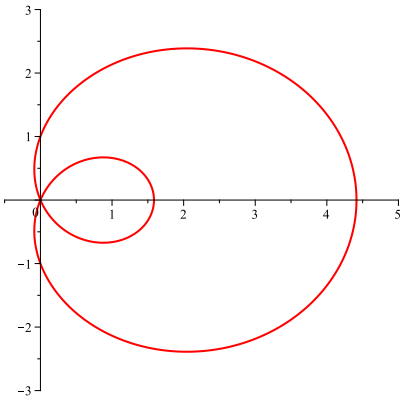

$s_{1,3}$=2, $s_{3,5}$=6, $s_{2,5}$=$s_{5,6}$ = 4

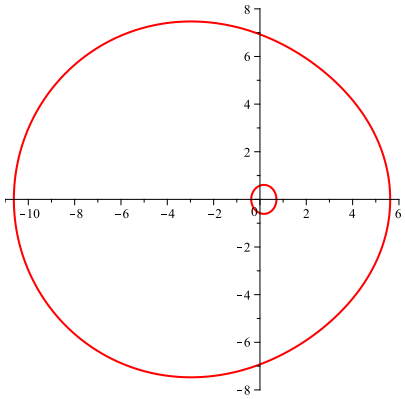

$s_{1,3}$=4, $s_{2,5}$=12, $s_{3,5}$=2, $s_{5,6}$ = 8

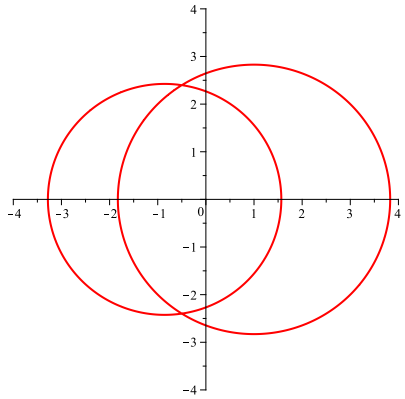

$s_{1,3}$=8, $s_{2,5}$=10, $s_{3,5}$=$s_{5,6}$ = 4

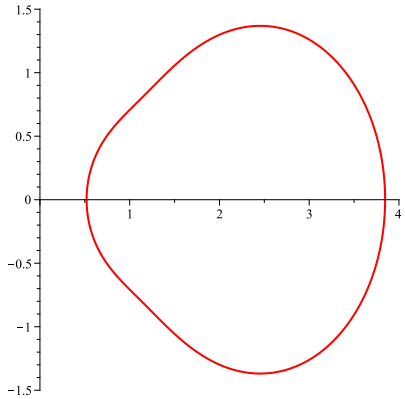

$s_{1,3}$=$\frac{1}{3}$, $s_{2,5}$=$\frac{5}{2}$, $s_{3,5}$=$\frac{5}{6}$, $s_{5,6}$ = $\frac{1}{2}$

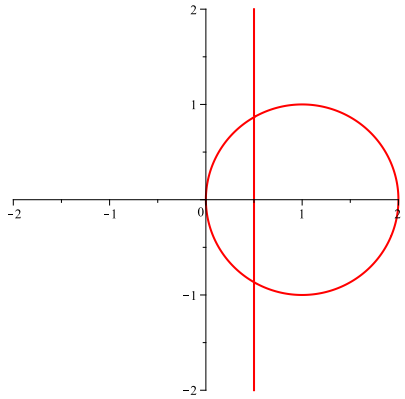

$s_{1,3}$=1, $s_{2,5}$=3, $s_{3,5}$=$s_{5,6}$ = 2

Figure 7: Examples of coupler curves generated by a scalene cell, a Peaucellier linkage with $s_{2,4} = s_{2,5}$, $s_{3,4} = s_{3,5}$, and $s_{4,6} = s_{5,6}$. The last example corresponds to a straight-line Peaucellier linkage.

If we replace them in equation (34), it simplifies to a expression of the form

$$(s_{3,4} - s_{3,5})^4 f(x, y) = 0. \tag{37}$$

Clearly, if $s_{3,4} = s_{3,5}$, the algebraic description of the curve traced by P_6 vanishes, thus indicating that the resulting mechanism has at least one branch of movement with more than one degree of freedom. However, in this case, $f(x, y)$ neither vanishes nor factorizes, thus indicating that there still is a single branch of movement in which P_6 traces a well-defined curve. The description of this curve actually reduces to the following bicircular quartic [12, Chapter 9]:

$$\beta_5 \left(x^2 + y^2\right)^2 + \beta_4 x \left(x^2 + y^2\right) + \beta_3 x^2 + \beta_2 y^2 + \beta_1 x + \beta_0 = 0, \tag{38}$$

where

$$\begin{aligned}
&\beta_5 = (1 - s_{1,3}),\\
&\beta_4 = \beta_1 = -2\,(1 + s_{2,5} - s_{3,5} - s_{1,3})\,,\\
&\beta_3 = \beta_2 + 4\,s_{2,5}\\
&\beta_2 = 1 - 2\,s_{1,3}(1 + s_{1,3}) + 2\,s_{3,5}(1 - s_{2,5}) - 2\,s_{5,6}(1 - s_{1,3}) + s_{1,3}^2 + s_{2,5}^2 + s_{3,5}^2,\\
&\beta_0 = (s_{2,5} - s_{5,6})^2\,(1 - s_{1,3})\,.
\end{aligned} \tag{39}$$

Fig. 7 presents some examples of this curve for different values of $s_{1,3}$, $s_{2,5}$, $s_{3,5}$ and $s_{5,6}$. This linkage was called by Cayley the scalene cell. It can be verified that the expression deduced by Cayley for this curve in [13] is equivalent to the one derived here.

The scalene cell is still a more general linkage than the celebrated straight-line Peaucellier linkage. This latter linkage can be seen as a scalene cell with the extra constraints

$$s_{3,4} = s_{4,6}, \text{ and } s_{1,2} = s_{1,3}. \tag{40}$$

By replacing (40) in (38), we obtain the equation

$$(y^2 + x^2 - 2\,x)(s_{5,6} - s_{2,5} + 2\,x) = 0. \tag{41}$$

This equation corresponds to a unit circle centered at P_1 and a line with equation $x = (s_{2,5} - s_{5,6})/2$ (see the last example appearing in Fig. 7).

6. Conclusions

A distance-based formulation to derive the closure polynomial of the Dixon linkage, relying only on elementary algebra, has been presented. One of the advantages of using distance-based formulations for obtaining closure polynomials is that, in general, it is easier to interpret the resulting expressions geometrically than by means of other formulations. For instance, we have shown how the conditions that made the leading coefficient factors vanish, either corresponding to the case in which the quadrilateral defined by four joints is orthodiagonal, or to the case in which the center of the circle defined by three joints is on the line defined by two other joints. We have also shown that each of the

factors of the independent coefficient, except one, falls within one of these two categories. The remaining factor, whose geometric interpretation remains elusive, deserves further study. The use of permutation groups to describe how all these factors are related to each other seems a promising line of investigation.

It has also been shown that the coupler curve of the generalized Peaucellier linkage is 11-circular of 22nd-degree, and how the bicircular quartic coupler curve expression of the scalene cell can be derived from it. The presented approach to obtain the coupler curve of the generalized Peaucellier linkage from the closure polynomial of the Dixon linkage can be applied to the analysis of coupler curves of other single-degree-of-freedom linkages. This is another point that deserves further attention.

References

[1] A. Dixon, On certain deformable frameworks, Messenger of Mathematics 29 (1900) 1–21.

[2] G. Laman, On graphs and rigidity of plane skeletal structures, Journal of Engineering Mathematics 4 (4) (1970) 331–340.

[3] W. Wunderlich, On deformable nine-bar linkages with six triple joints, Proceedings of the Koninklijke Nederlandse Akademie van Wetenschappen, Series A 79 (3) (1976) 257–262.

[4] H. Stachel, Higher-order flexibility for a bipartite planar framework, in: A. Kecskeméthy, M. Schneider, , C. Woernle (Eds.), Advances in Multi-Body Systems and Mechatronics, Inst. f. Mechanik und Getriebelehre der TU Graz, Duisburg, 1999, pp. 345–357.

[5] D. Walter, M. Husty, On a nine-bar mechanism, its possible configurations and conditions for flexibility, in: Proceedings of the 12th IFToMM World Congress in Mechanism and Machine Science, June 17 - 20, Besançon, France, 2007.

[6] N. Rojas, Distance-based formulations for the position analysis of kinematic chains, Ph.D. thesis, Institut de Robòtica i Informàtica Industrial (CSIC-UPC), Universitat Politècnica de Catalunya (2012).

[7] E. Dijksman, Motion Geometry of Mechanisms, Cambridge University Press, 1976.

[8] K. Menger, New foundation of euclidean geometry, American Journal of Mathematics 53 (4) (1931) 721–745.

[9] F. Thomas, N. Rojas, Pencils of dyads and Cayley-Menger determinants, in preparation.

[10] B. Hendrickson, Conditions for unique graph realizations, SIAM Journal on Computing 21 (1992) 65–84.

[11] T. Rainer, Rational families of circles and bicircular quartics, Ph.D. thesis, Friedrich-Alexander-Universität Erlangen-Nürnberg (2012).

[12] A. Basset, An Elementary Treatise on Cubic and Quartic Curves, Deighton, Bell and Company, 1901.

[13] A. Cayley, On the scalene transformation of a plane curve, Quarterly Journal of Pure and Applied Mathematics 13 (1875) 321–328.

List of Figures